

Eigenstates and dynamics of Hooke's atom: Exact results and path integral simulations

Hossein Gholizadehkalkhoran, Ilkka Ruokosenmäki, and Tapio T. Rantala

Citation: *Journal of Mathematical Physics* **59**, 052104 (2018); doi: 10.1063/1.5028503

View online: <https://doi.org/10.1063/1.5028503>

View Table of Contents: <http://aip.scitation.org/toc/jmp/59/5>

Published by the *American Institute of Physics*

PHYSICS TODAY

WHITEPAPERS

MANAGER'S GUIDE

Accelerate R&D with
Multiphysics Simulation

READ NOW

PRESENTED BY

 **COMSOL**

Eigenstates and dynamics of Hooke's atom: Exact results and path integral simulations

Hossein Gholizadehkalkhoran, Ilkka Ruokosenmäki, and Tapio T. Rantala
Physics, Tampere University of Technology, P.O. Box 692, FI-33101 Tampere, Finland

(Received 11 March 2018; accepted 24 April 2018; published online 11 May 2018)

The system of two interacting electrons in one-dimensional harmonic potential or Hooke's atom is considered, again. On one hand, it appears as a model for quantum dots in a strong confinement regime, and on the other hand, it provides us with a hard test bench for new methods with the "space splitting" arising from the one-dimensional Coulomb potential. Here, we complete the numerous previous studies of the ground state of Hooke's atom by including the excited states and dynamics, not considered earlier. With the perturbation theory, we reach essentially exact eigenstate energies and wave functions for the strong confinement regime as novel results. We also consider external perturbation induced quantum dynamics in a simple separable case. Finally, we test our novel numerical approach based on real-time path integrals (RTPIs) in reproducing the above. The RTPI turns out to be a straightforward approach with exact account of electronic correlations for solving the eigenstates and dynamics without the conventional restrictions of electronic structure methods. *Published by AIP Publishing.* <https://doi.org/10.1063/1.5028503>

I. INTRODUCTION

The problem of two electrons confined in a harmonic potential, sc. Hooke's atom, has been investigated by several authors.^{1–8} There are analytical solutions of the ground and excited states, but only for some specific confinement parameters or oscillator frequencies.¹ There are also some approximate and numerical approaches to solve the problem, but all of these are focused on the ground state energy and wave function of the three-dimensional system.^{8–13}

Solution of the problem can be reduced to those of center-of-mass (CM) and internal dynamics, and the latter one, further to radial and angular components. The radial component is the solution at the positive and negative parts of one-dimensional space, and thus, it turns out to form the solutions of one-dimensional Hooke's atom—analytically for the above-mentioned specific set of confinement parameters. These two parts can be combined to form symmetric and antisymmetric spatial wave functions as singlet and triplet (or bosonic and fermionic) states, respectively.

However, the one-dimensional Coulomb potential is not trivial to consider, and therefore, it has been a case of interest since 1959.¹⁴ It has been argued in many previous studies^{14–19} that only the odd wave functions are valid solutions of the Schrödinger equation. More recent studies on one dimensional strongly interacting confined quantum systems^{21–26} and previous studies on relativistic and non-relativistic one dimensional Coulomb potential^{14–20,27,28} motivate us to revisit the problem and demonstrate how to find solutions for all eigenstates and all confinement parameters both analytically and numerically.

Oseguera and de Llano²⁹ have proven that for the attractive one-dimensional Coulomb potential the singularity acts as an impenetrable barrier and space is divided into two independent domains. This is called the space splitting effect. Therefore, solutions for the positive and negative values of the relative coordinates of a two-particle system are completely independent. In one-dimension, the attractive delta function interaction and Coulomb interaction both cause the space splitting, too.²⁹

Due to the space splitting, the relative coordinate wave function of two particles should vanish at the origin. Extension of the problem to repulsive Coulomb potential is simple. It is enough to replace $-e^2 \rightarrow e^2$, and again, it can be shown similar to the attractive Coulomb interaction that the amplitude

of reflection coefficient for repulsive Coulomb interaction equals to one and the singularity acts as an impenetrable barrier.²⁹

In this study, we complete the numerous earlier studies by presenting solutions from the perturbation theory (PT) for all confinement parameters, and also, for both the ground state and excited states dynamics. We assess the accuracy of PT solutions as a function of confinement and order of PT. Our analytical PT results give better match with the exact numerical solutions in a strong confinement region as compared with interpolation formula in Ref. 1.

Furthermore, with a novel numerical approach based on Feynman path integral formalism in real time (RTPI),³⁰ we find wave functions, energetics, and dynamics of such a strongly correlated system to confirm the PT results and trends. We also assess the robustness of RTPI for excited states and dynamics, where it is applied for the first time.

In Sec. II, we introduce PT and RTPI for the one-dimensional confined charged particles. In Sec. III, we give the PT and RTPI solutions to Hooke's atom and assess the quality and accuracy by comparing with exact solutions for both eigenstates and quantum dynamics in an external time-dependent electric field.

II. MODEL AND METHODS

A. Separation of variables

The Hamiltonian of two electrons in a 3D harmonic well is

$$H = \frac{-\hbar^2}{2m_e} \nabla_1^2 + \frac{-\hbar^2}{2m_e} \nabla_2^2 + \frac{1}{2} m_e \omega^2 x_1^2 + \frac{1}{2} m_e \omega^2 x_2^2 + \frac{e^2}{|x_1 - x_2|}, \quad (1)$$

where x_1 and x_2 are the three coordinates of electrons 1 and 2, respectively. The relative and center of mass (CM) motion of the two electrons can be separated by defining new variables

$$r = x_1 - x_2$$

and

$$R = \frac{x_1 + x_2}{2}.$$

Now, the Hamiltonian separates as

$$H = H(r) + H(\ell) + H(R),$$

where $H(\ell) = \ell(\ell + 1)\hbar^2/2\mu r^2$ is the rotational part. For the rotational ground state of the relative motion ($\ell = 0$), one can rewrite the above Hamiltonian as follows:

$$\begin{aligned} H &= \frac{-\hbar^2}{2\mu} \frac{d^2}{dr^2} + \frac{1}{2} \mu \omega^2 r^2 + \frac{e^2}{|r|} + \frac{-\hbar^2}{2M} \nabla_R^2 + \frac{1}{2} M \omega^2 R^2 \\ &= H(r) + H(R), \end{aligned} \quad (2)$$

where $\mu = m_e/2$ and $M = 2m_e$ are the reduced and the total mass of electrons, respectively. If separating the wave function and total energy as $\psi(r, R) = \frac{u(r)}{r} \Phi(R)$ and $E_{\text{tot}} = E + E_{\text{CM}}$, then the CM motion is simple harmonic oscillation in all three dimensions

$$\frac{-\hbar^2}{2M} \frac{d^2}{dR^2} \Phi + \frac{1}{2} M \omega^2 R^2 \Phi = E_{\text{CM}} \Phi, \quad (3)$$

where $E_{\text{CM}} = (N + 1/2)\hbar\omega$ with non-negative integers N . Relative motion of the electrons is harmonic oscillation with the Coulomb interaction as a perturbation in the rotational ground state ($\ell = 0$),

$$-\frac{\hbar^2}{2\mu} u''(r) + \left(\frac{1}{2} \mu \omega^2 r^2 + \frac{e^2}{|r|} \right) u(r) = E u(r). \quad (4)$$

Equations (3) and (4) define the dynamics of 1D Hooke's atom without external fields. The solutions are bound states with quantized energies and those of the CM are states of a simple harmonic oscillator.

B. Perturbation theory

In this section, we review the PT and its applicability in one dimensional confined quantum systems with Coulomb potential as the interparticle interaction.

1. Reference states and boundary conditions

Equation (4) remains as the one dimensional Schrödinger equation to be solved. It would be natural to consider the Coulomb repulsion as perturbation and choose the harmonic oscillator as the reference system. However, in one-dimensional PT because of the space spitting effect, we are looking for solutions of relative motion with the boundary condition and symmetry like those of one-dimensional hydrogen atom at the origin^{14–19}

$$u(0) = 0. \quad (5)$$

This means that the odd numbered eigenstates of harmonic oscillator (4), only, are acceptable. Then, the exactly solvable problem with the same boundary condition as one dimensional Coulomb potential is³¹

$$-\frac{\hbar^2}{2\mu}\zeta_n''(r) + \frac{1}{2}\mu\omega^2 r^2 \zeta_n(r) = \epsilon_n \zeta_n(r), \quad (6)$$

where ζ_n are the eigenstates of one dimensional harmonic potential. The exact solutions are

$$\zeta_n(r) := \frac{\left(\frac{1}{\sqrt{\pi}}\sqrt{\xi}\right) \exp\left(-\frac{1}{2}\xi^2 r^2\right) H_n(\xi r)}{\sqrt{2^n n!}},$$

$$\epsilon_n = \left(n + \frac{1}{2}\right)\hbar\omega,$$

$$\xi = \sqrt{\frac{\mu\omega}{\hbar}},$$

$$n = 1, 3, 5, \dots$$

where H_n are the Hermite polynomials and only odd quantum numbers apply.

The integral solution of Eq. (4) can be written as³¹

$$u(r) = -\langle G(r, r') | \delta v(r') | u(r') \rangle, \quad (7)$$

$$\delta v(r') = \frac{e^2}{|r'|}, \quad (8)$$

where $G(r, r')$ is Green's function of Eq. (6) with the same boundary conditions as $u(r)$, i.e., Eq. (5). Using the eigenfunction expansion of Green's function, we have³¹

$$u_n = \zeta_n + \sum_{p \neq n} \frac{\langle \zeta_p | \delta v | u \rangle}{E_n - \epsilon_p} \zeta_p, \quad (9)$$

$$E_n = \epsilon_n + \langle \zeta_n | \delta v | u_n \rangle. \quad (10)$$

This is normal PT theory with odd numbered eigenstates. The validity condition ($\langle \zeta_n | \delta v | u_n \rangle \ll |E_n - E_{n\pm 1}|$) should also hold.³² We will discuss this in Sec. III.

C. Path integral approach

Recently, we have presented a novel real-time path integral (RTPI) approach to the electronic structure calculations and coherent quantum dynamics. It was first tested in the case of a single electron quantum dot.²⁸ Combined with Monte Carlo sampling of paths, RTPI was demonstrated to be a robust first-principles method and relatively simple to use, but computationally heavy.

Later, it was shown that in the case of Hooke's atom RTPI is capable of incorporating the electronic correlations exactly within numerical accuracy.³¹ Now, we demonstrate finding not only the ground state but lowest excited states, and also, dynamics as a response to external electric fields. We analyze the role of relevant approximations, the Monte Carlo method, and numerical parameters.

Thus, the RTPI is a general numerical method for testing the perturbation theoretical predictions, where analytical data are not available. Simultaneously, we can test the numerical performance and accuracy of RTPI for finding more complex many-particle wave functions and quantum phenomena, which are out of reach with the conventional first-principles methods.

The first and second excited states are calculated with the incoherent propagation path integral Monte Carlo^{30,33} simulations. The used parameters in atomic units are time step ($t = 0.1$), number of walkers ($N = 300\,000$), and the walker size ϵ ($\epsilon^2 = 0.005$). The purpose of the last parameter is to reduce the oscillations of the kinetic propagator. This is done by representing a single walker as a Gaussian function with variance ϵ^2 instead of Dirac delta function.³³

Here, it should be noted that the RTPI simulations are carried out in single-particle coordinates x_1 and x_2 , thus testing the performance of description of the electron correlations.

III. ONE DIMENSIONAL HOOKE'S ATOM

In this section, we discuss the solutions of one dimensional Hooke's atom within PT and RTPI. First we consider lowest stationary states, and then, dynamics in the presence of external time dependent electric field.

A. Stationary eigenstates

1. Ground state

Taut has introduced some exact solutions of 3D Hooke's atom for certain confinement parameters.¹ For the relative motion, this means solutions to the following Schrödinger equation [Eq. (9) in Ref. 1]:

$$-\frac{u''(r)}{2} + \frac{1}{2}\omega^2 r^2 u(r) + \frac{1}{r}u(r) = E_n u(r). \quad (11)$$

This is equivalent to the Schrödinger equation (4) for a particle with reduced mass ($\mu = 1$) and $\frac{1}{\sqrt{2}}$ electric charge. However, the approach involves finding solutions of two simultaneous equations, which restricts the answers to some specific values of ω and states.

Out of those we choose $\omega = 0.5$, because the analytical exact solution of the ground state is available for this value and it is also the largest one in the set of specified values of ω . In the first order PT, the energy levels as a function of n and ω can be written as

$$E_n = \left(2n + \frac{3}{2}\right)\hbar\omega + \frac{e^2 2^{-2n-1} \xi}{\sqrt{\pi}(2n+1)!} \int_{-\infty}^{\infty} \frac{e^{-(\xi x)^2} H_{2n+1}(\xi x)^2}{|x|} dx. \quad (12)$$

Where n is non-negative integers. The first term in Eq. (12) represents the simple harmonic oscillator energy levels with odd quantum number. Because of odd Hermite polynomials in the integrand, we are not worried about the singularity at origin. Thus, the first few energy levels are

$$\begin{aligned} E_0 &= 2e^2 \sqrt{\frac{\mu\omega}{\pi\hbar}} + \frac{3\omega\hbar}{2}, \\ E_1 &= \frac{5e^2}{3} \sqrt{\frac{\mu\omega}{\pi\hbar}} + \frac{7\omega\hbar}{2}, \\ E_2 &= \frac{89e^2}{60} \sqrt{\frac{\mu\omega}{\pi\hbar}} + \frac{11\omega\hbar}{2}, \\ E_3 &= \frac{381e^2}{280} \sqrt{\frac{\mu\omega}{\pi\hbar}} + \frac{15\omega\hbar}{2}. \end{aligned}$$

In Ref. 1, the interpolation method of eigenenergies is also presented. However, the fitting has been done for the confinement parameters in a narrow region, only. The maximum value of ω for the ground state is 0.5, and by increasing the number of states, the corresponding maximum ω decreases. Therefore, the extrapolation results for the ground state are accurate in region $\omega \leq 0.5$, for the first

excited state in region $\omega \leq 0.38$, and for higher states this region becomes narrower (cf. Table I in Ref. 1).

Rather than analytical exact solutions, there are two approximations in Ref. 1: the weak and the strong confinement approximations. As discussed in Ref. 33, for the largest confinement parameter ($\omega = 0.5$), the PT gives more accurate results compared to the weak and strong approximations.

A comparison between the analytical exact and perturbative solutions for $\omega \leq 0.5$ is shown in Fig. 1. The difference between these two decreases as n and ω increase, so the maximum difference appears for the ground state. For small values of ω , the PT is less accurate, because the validity condition for PT ($V_{nn} \ll |E_n - E_{n\pm 1}|$) is violated. We can use the average value of kinetic energy as a limit for the validity of PT. In the first order perturbative approximation, the average kinetic energy of relative motion for the ground state becomes negative for $\omega < \frac{4e^4\mu}{9\pi\hbar^3}$, which sets a minimum acceptable ω for the ground state in PT.

The ground state wave function and its properties have been discussed in detail in Ref. 33 already.

2. First two excited states

For the excited states with $\omega > 0.5$, the PT gives accurate results even in the first order. The accuracy of the PT results has been checked (up to fourth order) comparing the numerical exact solutions for the one-dimensional Hooke's atom.

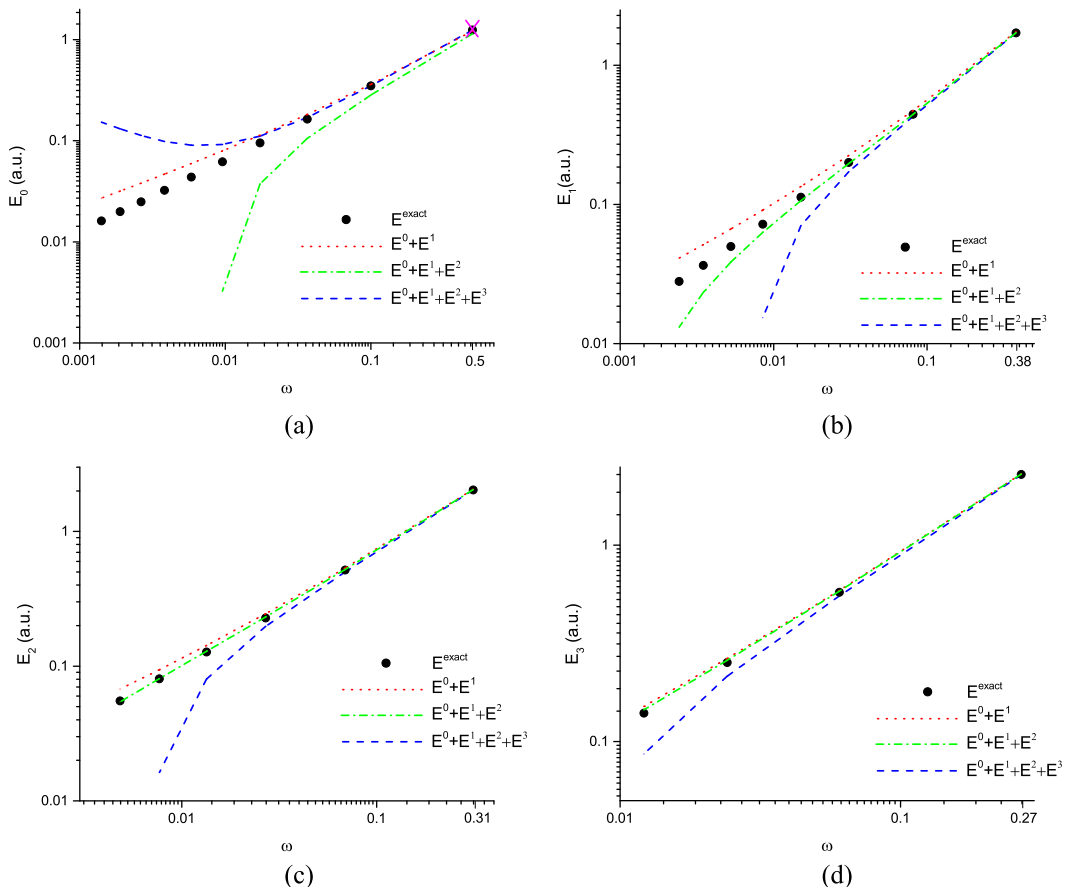


FIG. 1. Comparison of PT and analytical exact total energies (solid black circles) results in Ref. 1 of Hooke's atom in atomic units (hartree). The first-, second-, and third-order corrected energies are shown by the dotted (red), dotted-dashed (green), and dashed (blue) lines, respectively, and all axes are in logarithmic scale. (a) Ground state energy, $n = 0$ as a function of ω in logarithmic scales. The pink cross shows the RTPI result.³³ (b) First excited state, $n = 1$. (c) Second excited state, $n = 2$. (d) Third excited state, $n = 3$.

Figure 2 shows the relative errors between the first order PT and the numerical exact solution eigenenergies for the $\omega \geq 0.5$. As seen, even in the first order PT the relative errors reduce rapidly for excited states. The relative error for the ground state is around 5% and for states with $n \geq 3$, the relative errors are less than 1%.

We can compare the PT results for the first excited state of the relative motion with the analytical exact solution for $\omega = \frac{2}{5.26137}$. This ω has been chosen, because the analytical exact solution for the first excited state is available.¹ The analytical exact solution wave function for this frequency is¹

$$u_{1,\text{exact}} = Nr \exp\left(-\frac{\omega}{2}r^2\right)\left(r^3 - 36(r+4)r^2\omega + 12r^2 + 72r + 144\right), \quad (13)$$

where N is the normalization constant.

Comparison between the exact solution and PT solutions is given in Fig. 3. As expected, the first order PT has larger deviation from the exact solution, compared with the second and third order PT. Figure 3(b) shows the relative error between different order PT wave functions and exact solution.

Table I shows the results for the expectation values of Coulomb potential (V_c), relative motion harmonic potential ($V_{H,r}$), and relative motion kinetic energy (T_r). The total energy is the $E_{CM,0} + E_0$. The expectation values have been calculated directly from normalised wave functions. The RTPI energetics is in good match with the exact energies (and PT, where the analytical exact results are not available), but there is a systematic error where the electrons are close to each other ($r \rightarrow 0$) or when their separation is large. The former is due to the improved Trotter kernel approximation²⁸ with smaller error near the singular potential with finite time step. The latter is mostly caused by the small density of the Monte Carlo grid in that region and that error can be made smaller by increasing the number of walkers.^{30,33}

The first two excited states are combinations of the CM and relative motion ground states and first excited states. The first (second) excited state is a combination of the ground state of relative motion (CM) and excited state of CM (relative motion).

For the excited states, the results are reported for the $\omega = \frac{1}{2}$, because the analytical exact solution for the ground state is available for this frequency,¹ and the results can also be compared with the work on RTPI.³³ Using the Virial theorem for one dimensional harmonic oscillator, we have³²

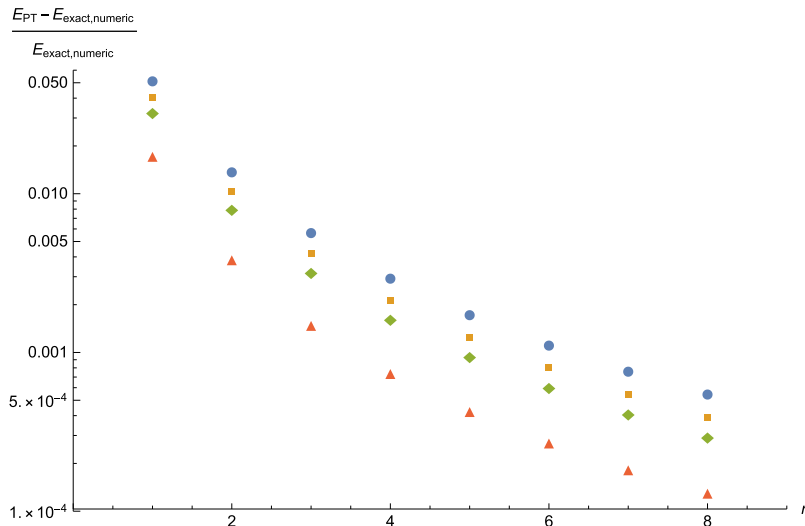


FIG. 2. The relative errors $(E_{PT} - E_{\text{exact,numeric}})/E_{\text{exact,numeric}}$ for the eigenenergies $n = 1, \dots, 8$ of Hooke's atom [$\omega = 0.5$ (blue circles), 0.7 (brown squares), 0.9 (green lozenges), and 2.0 (red triangles)]. The PT results in this figure are of the first order.

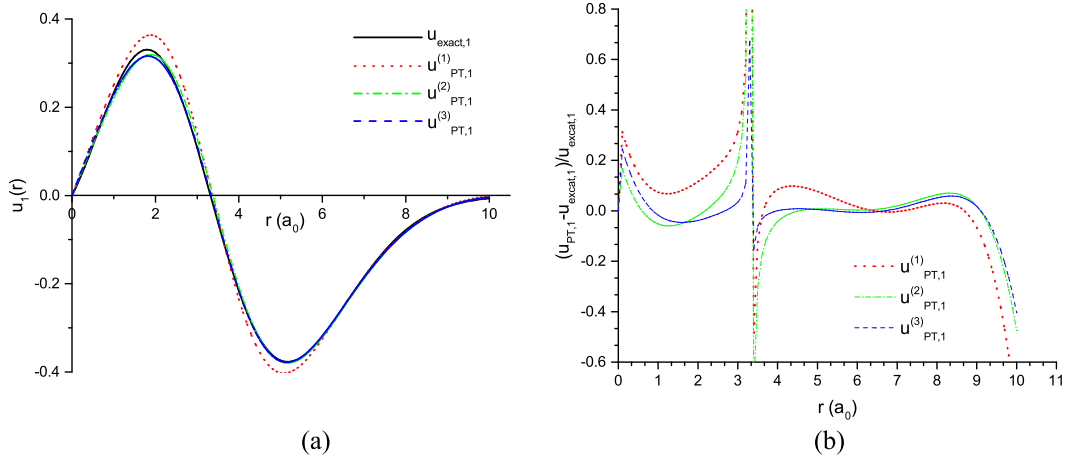


FIG. 3. (a) Comparison between the analytical exact solution (solid black line) and different order PT results for the first excited state wave function of relative motion ($\omega = \frac{2}{5.26137}$). $u_{PT,1}^{(n)}$ represents the n th-order corrections in PT. The first, second, and third order corrections are, respectively, shown by the dotted (red), dotted-dashed (green), and dashed (blue) lines. The relative error increases around the node and tail of the exact solution, where the wave function tends to zero. The horizontal axes represent relative distance between electrons in atomic units, i.e., bohr radius. (a) Analytical exact and different order PT wave functions. (b) Relative error between PT and analytical exact wave function.

$$\langle T_{CM} \rangle = \langle V_{H,CM} \rangle = \left(n + \frac{1}{2}\right) \frac{\hbar\omega}{2}, \quad (14)$$

where T_{CM} is kinetic energy of center of mass motion and $V_{H,CM} = \frac{1}{2}M\omega^2R^2$ is the CM harmonic potential. Here, for $n = 1$, this gives $3/8 = 0.375$. Table II shows the RTPI, PT, and analytical exact values (where available) for kinetic and potential energies of Hooke's atom. As one can see that the results are in agreement with exact solution results.

TABLE I. Expectation values of kinetic and potential energies of the first excited state in PT ($\omega = \frac{2}{5.26137}$) calculated directly from normalized wave functions. Comparison between the exact and PT wave functions is given in Fig. 3.

	Exact value	1st order PT	2nd order PT	3rd order PT
V_c	0.3521	0.3638	0.3452	0.3508
$V_{H,r}$	0.7671	0.7276	0.7832	0.7807
T_r	0.5912	0.6217	0.5845	0.5807
Total energy	1.9006	1.9032	1.9030	1.9024

TABLE II. The first excited state ($\omega = 0.5$) and its expectation values. The first excited state is the combination of first excited state of CM and ground state of relative motion.

	Exact value	RTPI	1st order PT	2nd order PT	3rd order PT
V_c	0.4474	0.4530(4) ^a	0.4354	0.4443	0.4466
$V_{H,r}$	0.5131	0.5117(1) ^a	0.5161	0.5218	0.5181
T_r	0.2894	0.2870(9) ^b	0.3028	0.2847	0.2861
$V_{H,CM}$	0.375	0.3722(1) ^a	0.375	0.375	0.375
T_{CM}	0.375	0.3765(15) ^b	0.375	0.375	0.375
Potential energy	1.3355	1.3369(3) ^b	1.3265	1.3412	1.3397
Total energy	2	1.9969(6) ^c	2.0043	2.0010	2.0009

^aPotential energy = $V_c + V_{H,r} + V_{H,CM}$ and its components are calculated as RTPI output.

^bThe expectation values of T_r and T_{CM} are calculated directly from normalized wave functions.

^cTotal energy has been calculated (independent from potential and kinetic energies) directly from the wave function's phase in RTPI.

TABLE III. The second excited state and its properties as Table II (cf. Fig. 4). The second excited state is combination of the CM ground state and first excited state of relative motion. Analytical exact values for this state are not available. The accuracy of the PT has been checked for the closest confinement parameter in Fig. 3(a) and Table I.

	Exact value	RTPI	1st order PT	2nd order PT	3rd order PT
V_c	...	0.4234(9) ^a	0.4233	0.4074	0.4119
$V_{H,r}$...	0.9811(9) ^a	0.9530	1.0074	1.0043
T_r	...	0.786(4) ^b	0.8159	0.7771	0.7753
$V_{H,CM}$	0.125	0.1620(3) ^a	0.125	0.125	0.125
T_{CM}	0.125	0.0986(7) ^b	0.125	0.125	0.125
Potential energy	...	1.5665(6) ^b	1.5013	1.5399	1.5413
Total energy	...	2.4331(2) ^c	2.4423	2.4420	2.4417

^aPotential energy = $V_c + V_{H,r} + V_{H,CM}$ and its components are calculated as RTPI output.

^bThe expectation values of T_r and T_{CM} are calculated directly from normalized wave functions.

^cTotal energy has been calculated (independent from potential and kinetic energies) directly from the wave function's phase in RTPI.

The energetics of the second excited state is shown in Table III. Clearly, for the second excited state, the average of T_r (relative motion kinetic energy), T_{CM} , and $V_{H,CM}$ from RTPI simulation is not well-fitted to the exact and PT results. This can be explained by the shape of the wave function. As one can see from Fig. 4, the RTPI predicts wider wave function comparing to the exact and PT. A wider wave function has smaller kinetic energy, and for the harmonic confinement, it gives larger potential energy. However, the total value of the eigenenergy and potential energy is in agreement with data from PT. Therefore, the different contributions balance each other in such way that the total quantities approach the correct values.

B. Dynamics in the presence of external transient field

Time evolution of the stationary states has been successfully simulated using RTPI in Ref. 33 already. As expected, there appears as change in the phase of the wave function only. To test the time evolution of Hooke's atom, a short time pulse of spatially constant electric field (linear in space and Gaussian in time) has been considered as a perturbation. We have chosen the external potential as

$$U(x, t) = \frac{U_0}{\sqrt{\pi\alpha}} x \exp\left(-\frac{(t-t_0)^2}{\alpha}\right), \quad (15)$$

where $U_0 = 1$, $\alpha = 0.1$, and $t_0 = 1$ (in atomic units).

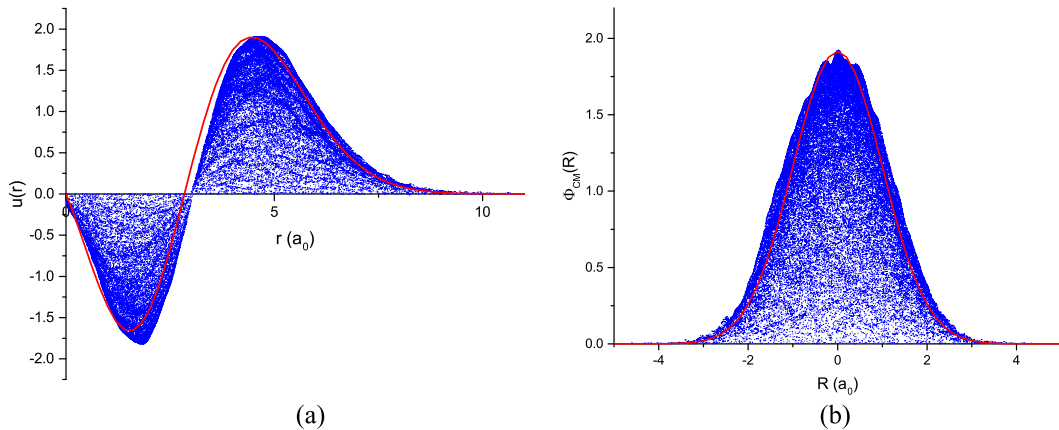


FIG. 4. A snapshot of the wave function from the converged RTPI simulation with $\Delta t = 0.1$, $N = 300\,000$, and $\omega = 0.5$ (blue walkers). Red line is an envelope curve from the 3rd order PT [cf. Fig. 3(a), $\omega \approx 0.38$] in (a) and exact solution from Eq. (3) in (b) fitted to the data. All the figures are in atomic units. (a) The first excited state of Internal motion. (b) Ground state of CM motion.

In the presence of this external electric field, the Hamiltonian of the system becomes as

$$\begin{aligned} H &= \frac{-\hbar^2}{2m_e} \nabla_1^2 + \frac{-\hbar^2}{2m_e} \nabla_2^2 + \frac{1}{2} m_e \omega^2 x_1^2 + \frac{1}{2} m_e \omega^2 x_2^2 + \frac{e^2}{|x_1 - x_2|} + U(x_1, t) + U(x_2, t) \\ &= H(r) + H(R) + 2U(R, t) \\ &= H(r) + H(R) + f(t)R, \end{aligned}$$

where $f(t) = \frac{2}{\sqrt{\pi}\alpha} \exp(-\frac{(t-t_0)^2}{\alpha})$.

1. Exact solution

As expected the spatially constant electric field does not change the internal motion and its effects appear only in CM motion. Therefore, in this subsection, we just discuss the CM motion. However, the RTPI solves the unseparated total wave function in single-particle coordinates again, and its results are presented in Subsection III B 2.

The Heisenberg equation of motion simplified into two coupled partial differential equations (PDE) can be written as

$$\begin{aligned} \frac{d}{dt} \langle R \rangle &= \frac{\langle P_{CM} \rangle}{M}, \\ \frac{d}{dt} \langle P_{CM} \rangle &= -(M\omega^2 \langle R \rangle + f(t)), \end{aligned} \quad (16)$$

where P_{CM} is the center of mass momentum. To find the average potential energy, we need $\langle R^2 \rangle$, which is found from the following coupled PDEs:

$$\begin{aligned} \frac{d}{dt} \langle R^2 \rangle &= \frac{2}{M} \left(\frac{\langle P_{CM}^2 \rangle}{M} - M\omega^2 \langle R^2 \rangle - f(t) \langle R \rangle \right), \\ \frac{d}{dt} \langle P_{CM}^2 \rangle &= -2M\omega^2 \left(\frac{\langle P_{CM} \rangle}{M} - M\omega^2 \langle R^2 \rangle - f(t) \langle R \rangle \right) - 2 \frac{d}{dt} \langle f(t) P_{CM} \rangle. \end{aligned} \quad (17)$$

Solution for $\langle R \rangle$ and $\langle P_{CM} \rangle$, give us the average of the potential energies as a function of time. Figure 5 shows the average of the total potential energy as a function of time.

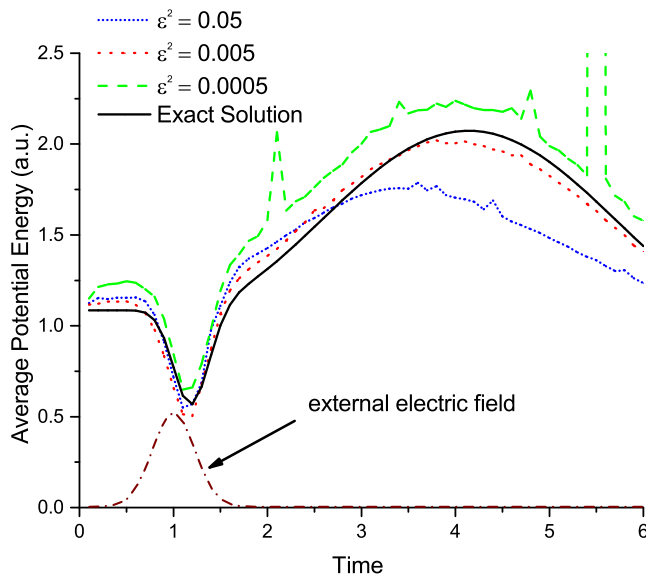


FIG. 5. Potential energy in atomic units from one MC simulation $\Delta t = 0.1$ and $N = 100\,000$ with different walker size ϵ in atomic units. Blue short dotted line $\epsilon^2 = 0.05$, red dotted line $\epsilon^2 = 0.005$, and green dashed line $\epsilon^2 = 0.0005$. The black solid line represents the exact solution.

2. Coherent RTPI simulation

In the time domain simulations, the ground state is affected by Gaussian shape pulse discussed above. As can be seen from the potential energies in Fig. 5, the walkers' size ϵ affects the results much more than in incoherent propagation. Too large ϵ cuts out higher energy states and results in incorrect energies (blue line) and too small ϵ increases in the incidental numerical error from the kinetic energy part of the propagator (green line). That is expected as it cuts out higher energy states, which are not present in the simulation of lower eigenstates but contribute to the real time evolution. For the real-time dynamics, ϵ must be chosen smaller than that for the optimal incoherent propagation.^{30,33} There is a delay in the system response to such an ultrafast transient process. It is due to the inertia of electrons. After the external pulse, the total energy is conserved and the electrons remain in harmonic oscillation.

Figure 6 shows the different interaction contributions in the potential energy. As expected, the Coulomb interaction remains unchanged during the time evolution, and the effects of the external electric field just appear in a short time interval.

3. Fourier transformation and time evolution

After the external pulse, the Hamiltonian of the system returns to its initial time independent form, but the wave function remains as a superposition of eigenstates of the unperturbed system,

$$\Psi(r, R, t) = \sum c_i \psi_i(r, R) e^{-i \frac{E_i t}{\hbar}},$$

where c_i depends on the matrix elements of the external potential. Therefore, the Fourier transform of Ψ is a sum of Dirac delta functions located at E_i . In practice, one can perform the Fourier transform by collecting finite samples of the wave function at different times and coordinates. Here the PT is used to find the time evolution for illustration of the approach. In the absence of analytical solutions, RTPI can be used to find the wave function time evolution.

Figure 7 shows the Fast Fourier Transformation (FFT) of the one dimensional Hooke's atom after applying the $U(x, t) + U(x^2, t)$ as the external potential. We choose a nonlinear perturbation $x + x^2$ because it has non-zero matrix elements for the first few excited states. The sampling rate is 100 (atomic units) and total integration time is 46 (atomic units). From Fig. 7, the eigenenergies are located at $\{1.5, 2.0, 2.43, 2.5, 2.93, 3.45\}$. Here we used $\Psi(1, 1, t)$ as the input in FFT.

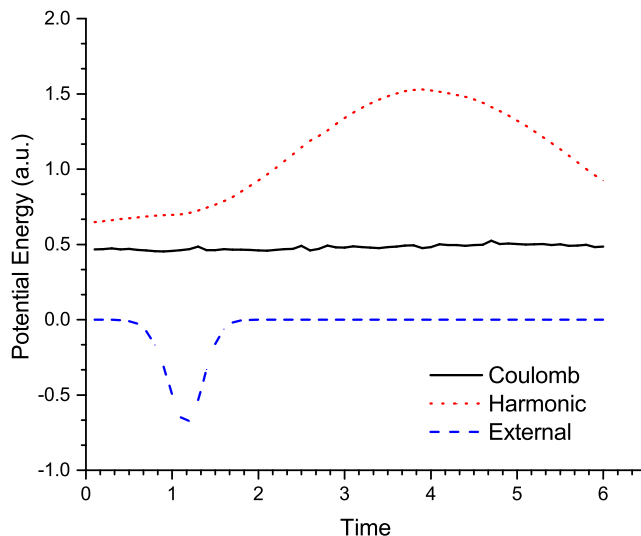


FIG. 6. Contributions to the potential energy in atomic units from Coulombic (black solid line), harmonic (red dotted line), and external potential (blue dashed line) effects from one MC simulation with $N = 100\,000$ and $\epsilon^2 = 0.005$.

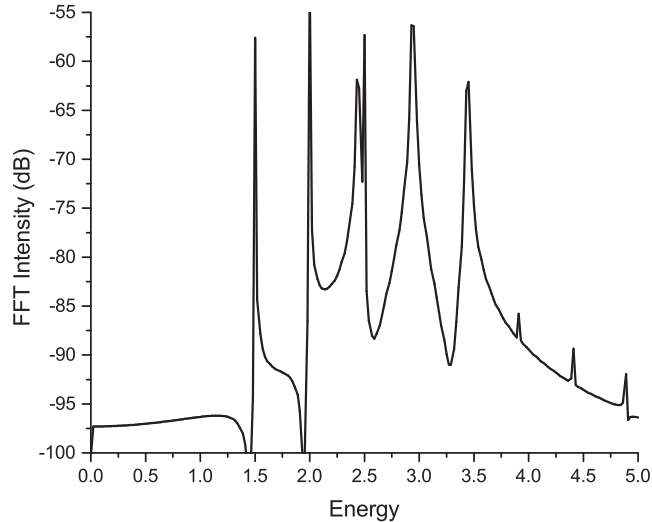


FIG. 7. Fast Fourier Transformation (FFT) of time dependent wave function of the one dimensional Hooke's atom. Peaks are located at 1.5, 2.0, 2.43, 2.5, 2.93, and 3.45. The small peaks at the end of energy axis come from numerical error.

IV. CONCLUSIONS

Hooke's atom has served as a well-defined model system, but also, as a challenging problem for decades.^{1–20} In addition to analytical approaches,^{1–8} numerical calculations have been published,^{1–14} and the specific challenges have arisen from the one-dimensional case and Coulomb space splitting, in particular.^{15–27} All of these studies, however, have considered the ground state, only.

In this study, we have been able to complete these numerous studies by including the excited states and dynamics induced by an external potential. We have shown how perturbation theory (PT) provides an accurate approach in the strong confinement regime, $\omega > 0.5$, and in particular, the real-time path integral (RTPI) approach with Monte Carlo simulation is a general and robust simulation tool^{28,31} for confined quantum systems. It should be mentioned here that similar studies could be carried out for other atoms with exact analytical solutions.^{34–36}

We have demonstrated that PT is accurate enough, even for higher excited states. This means that PT is probably suitable for studying the properties of the strongly one-dimensionally confined many body or few-body quantum systems.^{21–26} Unlike earlier analytical results, as described in Sec. III, PT is applicable for all confinement parameters and eigenstates.

With the RTPI, the improved Trotter kernel is shown to be useful with a large enough number of Monte Carlo walkers, in cases where exact propagators are not available. We find that the accuracy and stability of RTPI are tunable with the number of Monte Carlo walkers and the real time step size. Regarding ground states, the computational cost of RTPI is significantly higher than that of Diffusion Monte Carlo. However, one of the advantages of RTPI is that it provides one with the wave function explicitly, and thus, the evaluation of local multiplicative expectation values becomes straightforward. Moreover, as RTPI is capable of locating the nodal surfaces of excited states, it can be used to find the nodal surfaces in a diffusion Monte Carlo simulation of the excited states.

ACKNOWLEDGMENTS

The authors thanks the Tampere University of Technology for support.

¹ M. Taut, *Phys. Rev. A* **48**(5), 3561 (1993).

² U. Merkt, J. Huser, and M. Wagner, *Phys. Rev. B* **43**, 7320 (1991).

³ M. Taut, *Phys. Rev. B* **63**, 115319 (2001).

⁴ O. Ciftja, *Phys. Scr.* **88**, 058302 (2013).

⁵ H. Sprekeler, G. Kießlich, A. Wacker, and E. Scholl, *Phys. Rev. B* **69**, 125328 (2004).

- ⁶R. J. White and W. Byers Brown, *J. Chem. Phys.* **53**, 3869 (1970).
- ⁷G. W. Bryant, *Phys. Rev. Lett.* **59**(10), 1140 (1987).
- ⁸N. R. Kestner and O. Sinanoglu, *Phys. Rev.* **128**, 2687 (1962).
- ⁹D. Futai Tuan, *J. Chem. Phys.* **50**, 2740 (1969).
- ¹⁰P. M. Laufer and J. B. Krieger, *Phys. Rev. A* **33**(3), 1480 (1986).
- ¹¹J. M. Benson and W. Byers Brown, *J. Chem. Phys.* **53**, 3880 (1970).
- ¹²J. Cioslowski and K. Pernal, *J. Chem. Phys.* **113**, 8434 (2000).
- ¹³D. P. O'Neill and P. M. W. Gill, *Phys. Rev. A* **68**, 022505 (2003).
- ¹⁴R. Loudon, *Am. J. Phys.* **27**, 649 (1959).
- ¹⁵G. Palma and U. Raff, *Can. J. Phys.* **84**, 787–800 (2006).
- ¹⁶D. P. O'Neill and P. M. W. Gill, *J. Chem. Phys.* **122**, 094110 (2005).
- ¹⁷L. K. Haines and D. H. Roberts, *Am. J. Phys.* **37**, 1145 (1969).
- ¹⁸A. N. Gordeyev and S. C. Chhajlany, *J. Phys. A: Math. Gen.* **30**, 6893 (1997).
- ¹⁹H. N. Nunez-Yepe, A. L. Salas-Brito, and D. A. Solis, *Phys. Rev. A* **83**, 064101 (2011); **89**, 049908(E) (2014).
- ²⁰H. N. Spector and J. Lee, *Am. J. Phys.* **53**, 248 (1985).
- ²¹A. G. Volosniev, D. V. Fedorov, A. S. Jensen, M. Valiente, and N. T. Zinner, *Nat. Commun.* **5**, 5300 (2014).
- ²²X.-W. Guan *et al.*, *Phys. Rev. Lett.* **111**, 130401 (2013).
- ²³Xi-W. Guan *et al.*, *Rev. Mod. Phys.* **85**, 1633 (2013).
- ²⁴Y.-a. Liao *et al.*, *Nature* **467**, 567 (2010).
- ²⁵T. Kinoshita, T. Wenger, and D. S. Weiss, *Science* **305**, 1125 (2004).
- ²⁶B. Paredes *et al.*, *Nature* **429**, 277 (2004).
- ²⁷W. Fischer, H. Leschke, and P. Müller, *J. Phys. A: Math. Theor.* **40**, 1011 (2007).
- ²⁸C. A. Downing and M. E. Portnoi, *Phys. Rev. A* **90**, 052116 (2014).
- ²⁹U. Oseguera and M. de Llano, *J. Math. Phys.* **34**, 4575 (1993).
- ³⁰I. Ruokosenmäki and T. T. Rantala, *Commun. Comput. Phys.* **18**, 91 (2015).
- ³¹P. McCord Morse and H. Feshbach, *Methods of Theoretical Physics* (McGraw-Hill, 1953), Vol. 2.
- ³²L. D. Landau and E. M. Lifshitz, *Quantum Mechanics: Non-Relativistic Theory* (Elsevier, 1981).
- ³³I. Ruokosenmäki *et al.*, *Comput. Phys. Commun.* **210**, 45 (2017).
- ³⁴M. Moshinsky, *Am. J. Phys.* **36**, 52 (1968).
- ³⁵R. Crandall, R. Whitnell, and R. Bettega, *Am. J. Phys.* **52**, 438 (1984).
- ³⁶C. A. Downing, *Phys. Rev. A* **95**, 022105 (2017).